ELSEVIER

Applied Surface Science 200 (2002) 150–164

applied surface science

www.elsevier.com/locate/apsusc

# Multifunctional ToF-SIMS: combinatorial mapping of gradient energy substrates

Sonya V. Roberson[a,*], Albert J. Fahey[a], Amit Sehgal[b], Alamgir Karim[b]

[a]*Surface and Microanalysis Science Division, National Institute of Standards and Technology, 100 Bureau Drive, Stop 8371, Gaithersburg, MD 20899-8371, USA*

[b]*Polymers Division, National Institute of Standards and Technology, 100 Bureau Drive, Stop 8542, Gaithersburg, MD 20899-8542, USA*

Received 20 December 2001; accepted 27 June 2002

**Abstract**

We present a simple method for chemical modification of chlorosilane self-assembled monolayers (SAMs) on Si surfaces by exposure to a gradient of UV-ozone radiation to create stable substrates with a range of contact angles ($\theta_{H_2O} \approx 5$–$95^\circ$) and surface energies on a single substrate. These gradient energy substrates are developed to potentially generate libraries for combinatorial studies of thin film phenomenology, where a systematic variation of interfacial surface energy represents one of the significant parameters along one axis. The graded oxidation process presents a systematic variation of surface chemical composition. We have utilized contact angle measurements and time-of-flight secondary ion mass spectrometry (ToF-SIMS) to investigate this variation for a series of ions, among which are $SiCH_3^+$, $SiOH^+$ and $COOH^-$. We show that the macroscopic measurements of surface free energy/contact angle correlate with the detailed analysis of surface chemistry (as assessed by ToF-SIMS) on these test substrates.
© 2002 Elsevier Science B.V. All rights reserved.

*PACS:* 82.80.ms (Mass spectrometry); 81.65.-b (Surface treatments)

*Keywords:* Surface energy gradient; ToF-SIMS; UV-ozone treatment

## 1. Introduction

Combinatorial methods in chemistry and the pharmaceutical sciences have traditionally explored inorganic [1–6] and organic [7–10] synthesis of large collections (libraries) of compounds, which are then tested for particular physical and chemical properties. This technology has significantly increased the efficiency of drug and material discovery and necessitates the development of high-throughput screening/analysis techniques [11]. The extension of combinatorial methods to materials science has resulted in a shift in emphasis from screening for ''hits'' and the design of molecular structures (as in drug discovery) to knowledge discovery obtained by rapidly exploring multivariable-parameter space and investigating how those variables (compositional, processing, etc.) affect phenomenological physics. Micro- and nanoscale patterning and continuous gradients in surface chemistry modifications

* Corresponding author. Tel.: +1-301-975-3798; fax: +1-301-417-1321.
*E-mail address:* sonya.roberson@nist.gov (S.V. Roberson).

0169-4332/02/$ – see front matter © 2002 Elsevier Science B.V. All rights reserved.
PII: S0169-4332(02)00887-5

[12,13] are being used to generate libraries having a systematic variation of surface properties. These libraries provide multi-parameter spaces to study interfacial phenomena in thin films, adhesion and biocompatibility.

Surface free energy is one property that is exploited in creating such libraries. A novel method of creating surface free energy gradients using UV-ozone (UVO) treatment has been developed. In the UVO photo-oxidation method, a surface is exposed to short-wavelength (184.9 and 253.7 nm) UV radiation. Molecular oxygen is dissociated by the 184.9 nm radiation and ozone by the 253.7 nm radiation. Atomic oxygen is simultaneously generated during these dissociations. We have utilized UVO exposure through variable density filters to generate silane monolayers with continuous free energy gradients. This treatment introduces a range of functionalities to the surface. Among these are carboxylate, carbonyl and other oxygenated functionalities [14,15]. The ensuing changes in free energy (as assessed in terms of surface wettability) that result from the addition of these polar functional groups were evaluated using contact angle measurements. In this study, we used time-of-flight secondary ion mass spectrometry (ToF-SIMS) to investigate the relationship between contact angle/surface free energy changes and the functional groups present on the surface of two different silane monolayers. ToF-SIMS is a surface analytical technique that is capable of detecting elemental and molecular species with a spatial resolution of <1 μm. Because of these characteristics, and the imaging capabilities of ToF-SIMS, the technique is ideal for compositional analysis of these and other combinatorial arrays. The SIMS spectra reveal that UVO exposure introduces a variety of modifications to the silane surfaces. The trends associated with these modifications and their relationship to surface hydrophilicity will be discussed.

## 2. Experimental

### 2.1. Materials

The monofunctional *n*-octyldimethylchlorosilane (ODS; >95% mass concentration; $M_w = 206.83$; bp 222.5 °C) was purchased from Gelest Inc. (Tullytown, PA).[1] The octyltrichlorosilane (OTS; 97% mass concentration; $M_w = 247.67$; bp 233 °C) was purchased from Aldrich. The alkylchlorosilanes were received and stored under nitrogen. Solutions with a mass fraction of 2.5% of the alkylchlorosilanes in toluene (Mallinckrodt, 99.9%) were used. The silicon wafers used for substrates (n-type, 400–500 μm thick, <1 0 0> orientation) were purchased from Wafer World Inc.

The Si wafers were cleaved into rectangular substrates (~4.5 cm × 3 cm) and subsequently washed with detergent, thoroughly rinsed with deionized water, and treated with UV-ozone plasma for 10 min to grow an oxide layer and clean absorbed organics. The substrates were subsequently treated with buffered oxide etch (7:1 CMOS$^{TM}$ grade, J.T. Baker) to strip the layer of oxide. The substrates were then treated with UV-ozone plasma again for 3 min to re-grow the oxide layer. These steps were taken for consistency of growing the same thickness of oxide layer for all the experiments. The dry substrate was then submerged for 45 min in 40 ml of a 2.5% mass fraction solution of the alkylchlorosilane in toluene in a clean glass petri dish. The petri dish was previously treated with the chlorosilane to protect the glass and the solution was covered under a blanket of $N_2$ to exclude moisture from air. The direct nucleophilic attack on the chlorosilane by the silanols present on the surface results in a strong covalent bond to the surface. The wafers were rinsed with copious amounts of toluene and then baked in a vacuum oven (at 120 °C) for at least 1 h to dry the octylsilane monolayer on the Si substrate.

### 2.2. UV-ozone (UVO) treatment of SAMs

The monolayers were exposed to a gradient of UV-ozone radiation through a variable density filter. The variable density filter was custom designed by Maier Photonics with vapor deposited inconel (Ni, Cr, Fe alloy) on a 5.08 cm × 2.54 cm (±0.03 cm) × 1.5 mm thick fused silica substrate. The optical density varied

[1] Certain commercial equipment, instruments or materials are identified in this paper in order to specify adequately the experimental procedure. Such identification does not imply recommendation or endorsement by the National Institute of Standards and Technology, nor does it imply that the materials or equipment identified are necessarily the best for the purpose.

from 0.04 to 1.0 (measured at 330 nm) across the fused silica in 11 steps of 4 mm giving a linear gradient in the intensity of the incident UV radiation at the surface. The filter was placed with a spacing of ≈500 μm from the surface to allow oxygen to diffuse across the sample. The atomic oxygen, generated in close proximity to the surface by the UV radiation, oxidizes the organic alkylsilane layer. The molar concentration of this atomic oxygen should be directly proportional to the incident UV intensity, which in turn systematically varies the rate of oxidation across the surface. The systematic variation of the extent of oxidation of the organic layer in turn changes the surface free energy across the sample. The self-assembled monolayer was exposed to the UV-ozone treatment in a Jelight UVO-Cleaner® (Model 42), which is typically used for decontamination of surgical tools. The UV source is a low-pressure mercury vapor grid lamp. The apparatus' simplicity and availability for generating reproducible gradients in surface energy make it a powerful tool for studying polymer physics in thin films combinatorially. The mono- and trichlorosilane layers were exposed to UV-ozone radiation for 5 min. The monolayers were immediately transferred to the SIMS instrument for surface characterization. Separate, but simultaneously prepared, samples were used for contact angle measurements and for SIMS analyses.

### 2.3. Contact angle measurements

Static contact angle measurements for water (deionized; resistivity ∼18 MΩ) and methylene iodide (99%, Aldrich) were performed at room temperature with a Kruss G2 contact angle measuring system. This multiple fluid dispensing system allows for programmed deposition of known volume droplets of a chosen fluid (pre-loaded into the dispensing syringe mechanism; maximum of six) at any two dimensional ($x$ and $y$) spatial coordinate. The system automatically takes a profile image of a known volume of the droplet of a chosen fluid at a known coordinate and fits the droplet shape to determine the contact angle ($\theta$) by known methods (Young–Laplace, tangent method, etc.). Small droplet volumes of 1.5 μl were used to minimize the effect of gravity on the measurements.

### 2.4. X-ray reflectivity measurements

Preliminary X-ray reflectivity measurements were performed on Philips X-pert™ instrumentation for the monochlorosilane sample prepared by the above procedure. The reflectivity profiles fit a model of an oxide layer ($SiO_x$) with a roughness of 0.5 nm covered by a monolayer of 1 nm of dimethyloctylsilane. Detailed measurements will be included elsewhere. These preliminary measurements confirm a near monolayer coverage of the substrate, with the height of the SAM layer (1 nm) determined to be less than fully stretched packed ODS (≈12 Å).

### 2.5. SIMS measurements

#### 2.5.1. Spectra

Positive and negative static SIMS analyses were performed with the ToF-SIMS IV (Ion-ToF, Münster, Germany). Spectra were generated with a pulsed 9 keV argon ion beam (≈2 pA target current) and were collected in 150 μm × 150 μm areas along the length of the rectangular sample. Each automated spectral acquisition required 300 s. These conditions resulted in doses that were well below the static SIMS limit of $10^{13}$ ions/cm$^2$. A pulsed, low energy (≈30 eV) electron flood gun was used for charge neutralization. Automated acquisition of the spectra was achieved by using the Microsoft Dynamic Data Exchange (DDE) protocol from within a Python script to control Ion-ToF's spectral acquisition program and the Raith ESCOSY® stage control software. The Python script would start the acquisition of a spectrum at a particular analysis position, save it with a unique file name and then step the stage to the next analysis position. Forty to eighty spectra were collected over periods of 4–8 h. (Data collection was started on the most hydrophilic end of the sample.) Once the data were collected, analysis was performed with the IonSpec® software or by means of a custom program. The IonSpec® analyses were performed with the Peak Evaluation and Peak List utilities in the program. The custom program was capable of extracting the secondary ion intensities of any peaks chosen by the operator. Specifically, $O^-$, $C_3^-$, $COOH^-$, $SiCH_3^+$, $SiOH^+$, and $Si_2O^+$ were chosen for the current analysis. Since the high-mass-resolution measurements spanned 40 mm of

the sample surface over several hours, a recalibration of the mass scale was performed for each spectrum. This recalibration was achieved by having the operator specify peaks (such as H and Si) for the recalibration so that the program could re-center on those peaks (under the assumption that the peaks had shifted only a small amount) and calculate a new mass scale calibration.

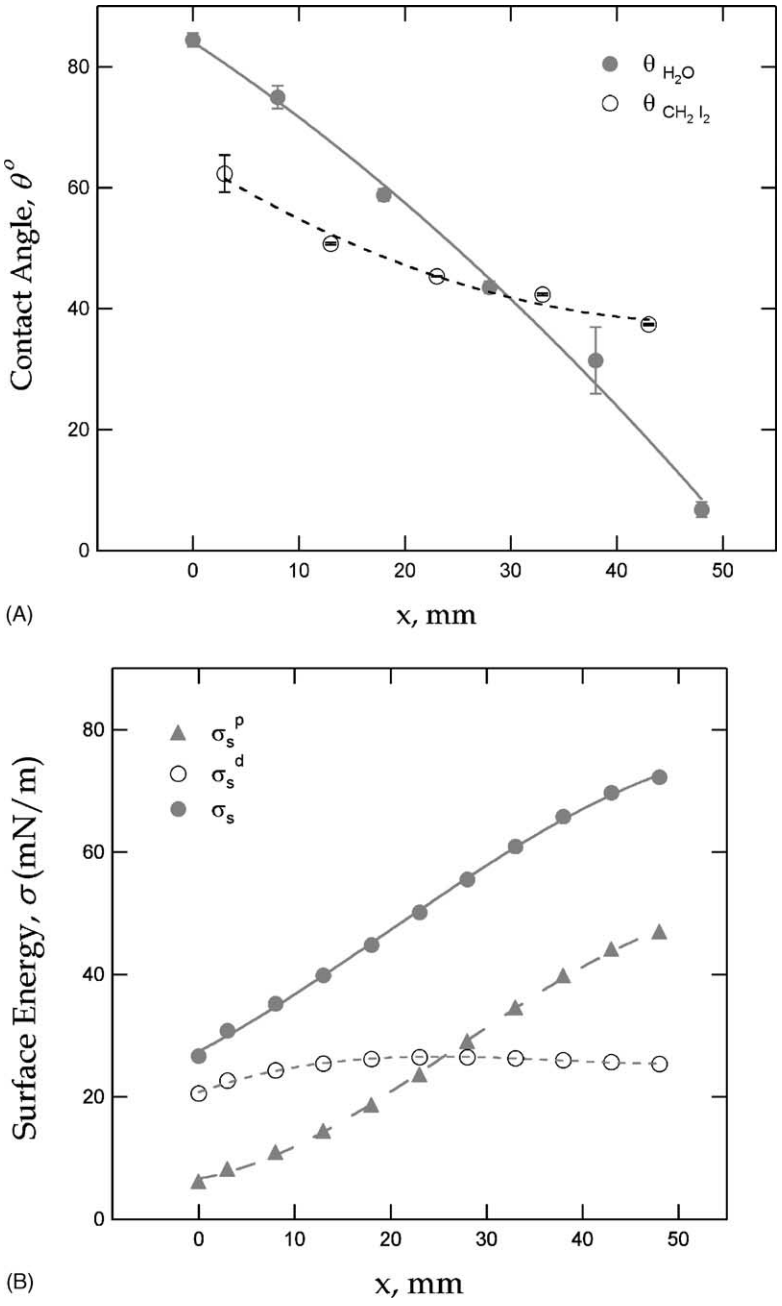


Fig. 1. (A) Contact angle measurements for an ODS monolayer. (B) Estimated spatial variation of the total surface energy ($\sigma_s$, ●), and the polar ($\sigma_s^p$, ▲) and the dispersive ($\sigma_s^d$, ○) contributions along the $x$-axis for an ODS monolayer.

*2.5.2. Imaging*

Secondary ion images were acquired with a 25 keV $Ga^+$ primary ion beam. The target current was approximately 2 pA. The $Ga^+$ beam was rastered over 500 μm × 500 μm areas containing 128 × 128 pixels. Acquisition times ranged from 534 to 1047 s, with total ion doses of 2–4 × $10^{12}$ ions/$cm^2$.

## 3. Results and discussion

### 3.1. Contact angle measurements

The contact angles vary from 6.8 to 84.5° (Fig. 1A), corresponding to surface energy ranging from 72 to 27 mN/m. The water contact angle for unirradiated ODS and OTS monolayers was ≈93°, corresponding to a surface energy of 26 mN/m.

UVO treatment resulted in a systematic variation in surface chemistry across the substrate. There was a steady increase in the hydrophilic nature of the surface (increase in surface energy) with increasing UVO exposure. As will be shown in the following sections, an enhancement in the polar surface species resulted from increased UVO treatment. The systematic gradient in surface functionality was conveniently measured by an array of droplets of $H_2O$ and $CH_2I_2$ placed on the substrate. The spatially resolved $\theta_{H_2O}$ and $\theta_{CH_2I_2}$ (Fig. 1A, calculated for identical UV-ozone exposure) were used to estimate the gradient in substrate surface energy ($\sigma_s$) by the Good and Girifalco geometric mean approximation method (GMA method) [16,17]. The method involves the use of known values of the polar and the dispersive components ($s_i^p$ and $\sigma_i^d$, respectively) of the surface free energy of at least two known fluids and the measurement of the contact angles on the substrate. Simultaneous solution of equilibrium interfacial interaction equation $(1+\cos\theta_i)\sigma_i = 2(\sigma_i^d\sigma_s^d)^{0.5} + 2(\sigma_i^p\sigma_s^p)^{0.5}$ yields values for $\sigma_s^d$ and $\sigma_s^p$. The variation of the calculated surface energy with position is plotted in Fig. 1B. The GMA method affords resolution of total surface ($\sigma_s = \sigma_s^p + \sigma_s^d$) and the polar and dispersive component ($\sigma_s^p$ and $\sigma_s^d$), respectively. Fig. 1B shows the similar trends for the variation of $\sigma_s^p$ and the total $\sigma_s$, while the dispersive component remains constant. This result is expected, since the chemical modification of the alkyl SAMs contributes to only the short-range polar interactions while the long-range dispersions are constant. Multiple samples were prepared to verify the reproducibility of the UVO gradient method for different radiation dosages achieved by varying the exposure times [18]. Under identical conditions of SAM preparation and UVO exposure similar ranges of water contact angles $\theta_{H_2O}$ (±2°) were obtained. For any given exposure condition the water contact angle may be correlated to a substrate surface energy, with the multiple data sets collapsing onto a single master-curve of $\sigma \sim F(\theta)$

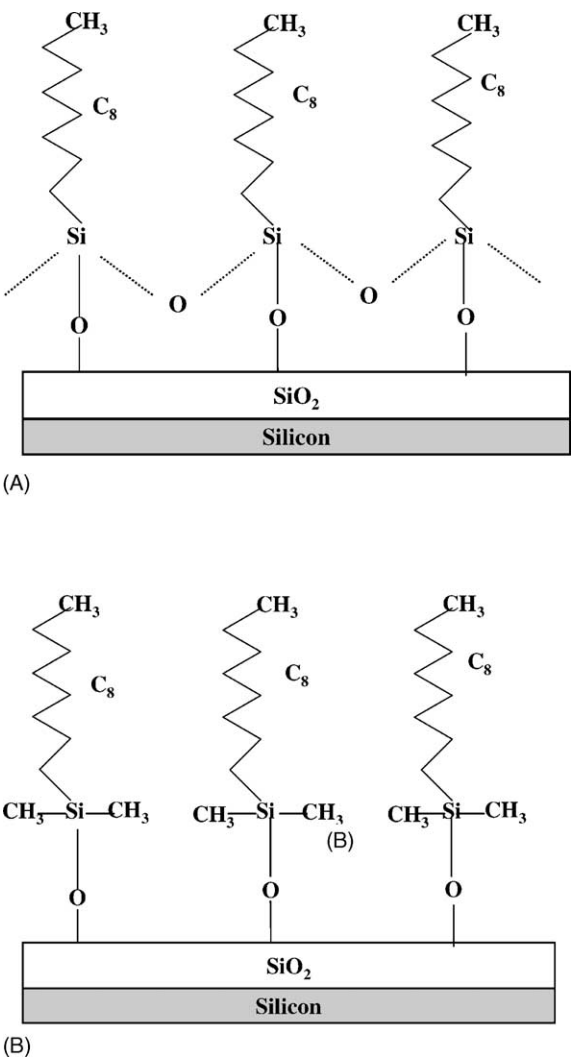


Fig. 2. Schematic diagrams of (A) OTS and (B) ODS monolayers.

which may be parametrically described by a simple polynomial.

### 3.2. Survey spectra

Schematic diagrams of the model surfaces are illustrated in Fig. 2. UVO exposure is expected to cause fragmentation of molecular bonds and to increase the polarity of the surfaces through addition of oxygen atoms [14,19]. Before analyzing the UVO gradient samples, positive (Fig. 3) and negative (Fig. 4) ToF-SIMS spectra of unirradiated silane monolayers were obtained. These spectra were compared with those obtained from monolayers which had been exposed to UVO treatment (no variable density filter) for 5 min. Our goal was to identify spectral variations resulting from this treatment. These variations were then monitored during analysis of the gradient samples.

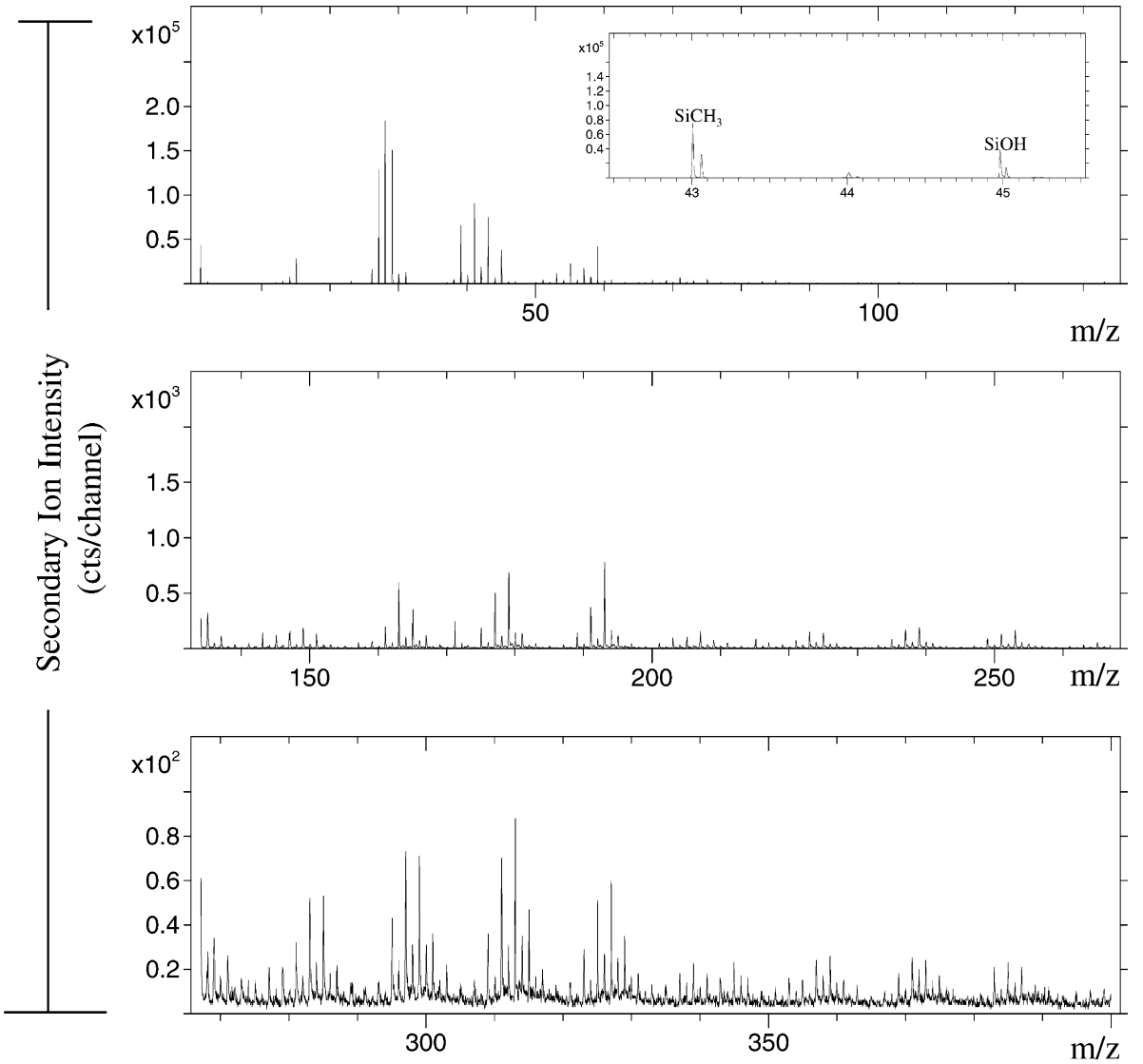


Fig. 3. High-mass-resolution positive ion SIMS spectrum of an unirradiated ODS monolayer. The inset shows the peak intensities for $SiCH_3^+$ ($m/z$ 43) and $SiOH^+$ ($m/z$ 45).

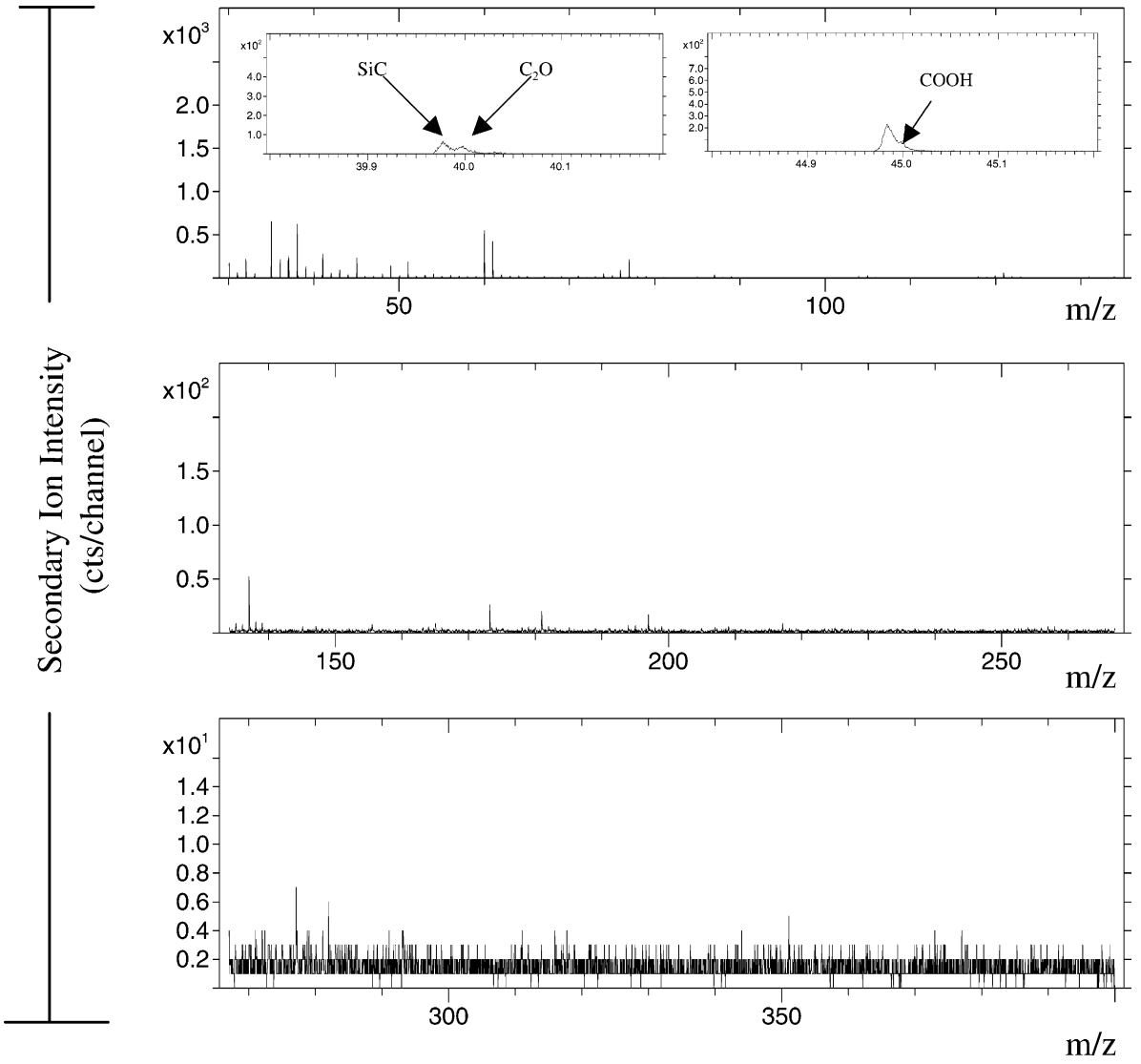


Fig. 4. High-mass-resolution negative ion SIMS spectrum of an unirradiated OTS monolayer. The inset shows the peak intensities for $SiC^-$ and $C_2O^-$ (*m*/*z* 40) and $COOH^-$ (*m*/*z* 45).

The positive and negative ion trends shown apply to both systems (ODS and OTS).[2] Fig. 5 shows the positive ion spectrum for the ODS monolayer after UVO treatment. A comparison of this spectrum and the spectrum shown in Fig. 3 indicates that the secondary ion signal for $SiCH_3$ (*m*/*z* 43) is reduced upon UVO irradiation. In addition, the signal for SiOH (*m*/*z* 45) is increased. Likewise, upon comparing the negative ion spectrum of irradiated OTS (Fig. 6) with Fig. 4, we observed that the secondary ions signals for SiC and $C_2O$ (*m*/*z* 40) decrease and increase, respectively, upon UVO irradiation. The relative intensities of the peaks at *m*/*z* 45 also change. One of these peaks has been identified as COOH. The reduction in the

[2] In the negative spectrum of unirradiated ODS a very weak signal was observed at *m*/*z* 187. This signal is attributed to the molecular ion (the octyldimethylsiloxy anion), and was further diminished by UVO treatment. No molecular ion signal was obtained for either the unirradiated or the irradiated OTS monolayer.

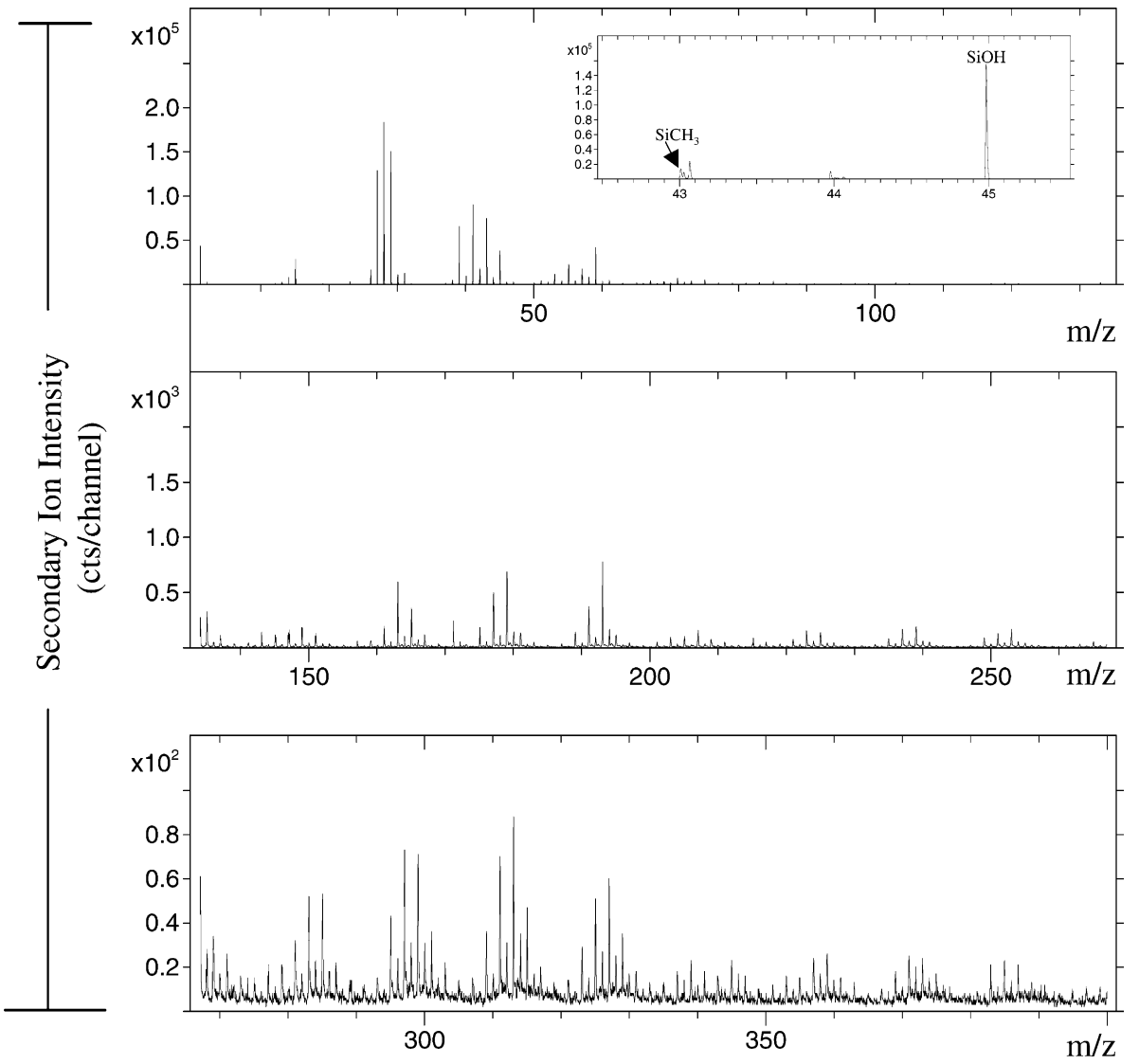


Fig. 5. High-mass-resolution positive ion SIMS spectrum of an irradiated ODS monolayer. The inset shows the peak intensities for $SiCH_3^+$ (*m*/*z* 43) and $SiOH^+$ (*m*/*z* 45).

$SiCH_3^+$ and $SiC^-$ signals is expected due to fragmentation of the silane overlayer during UVO exposure [20]. Similar findings were reported for other surface modifications techniques, such as X-ray and ion beam modification [21,22]. The increase in the signal for $C_2O^-$ is attributed to cross-linking between the hydrocarbon chains [23]. The enhancement in the signals observed for the polar species, $COOH^-$ and $SiOH^+$, is also expected as the levels of photo-oxidation increases. $Si_2O^+$ and $C_3^-$ also showed variations in secondary ion intensity upon UVO exposure. The nature of these variations will be addressed in Sections 3.3 and 3.4.

### 3.3. Combinatorial analysis

Fig. 7 shows the positive secondary ion trends observed for the ODS monolayer gradient surface

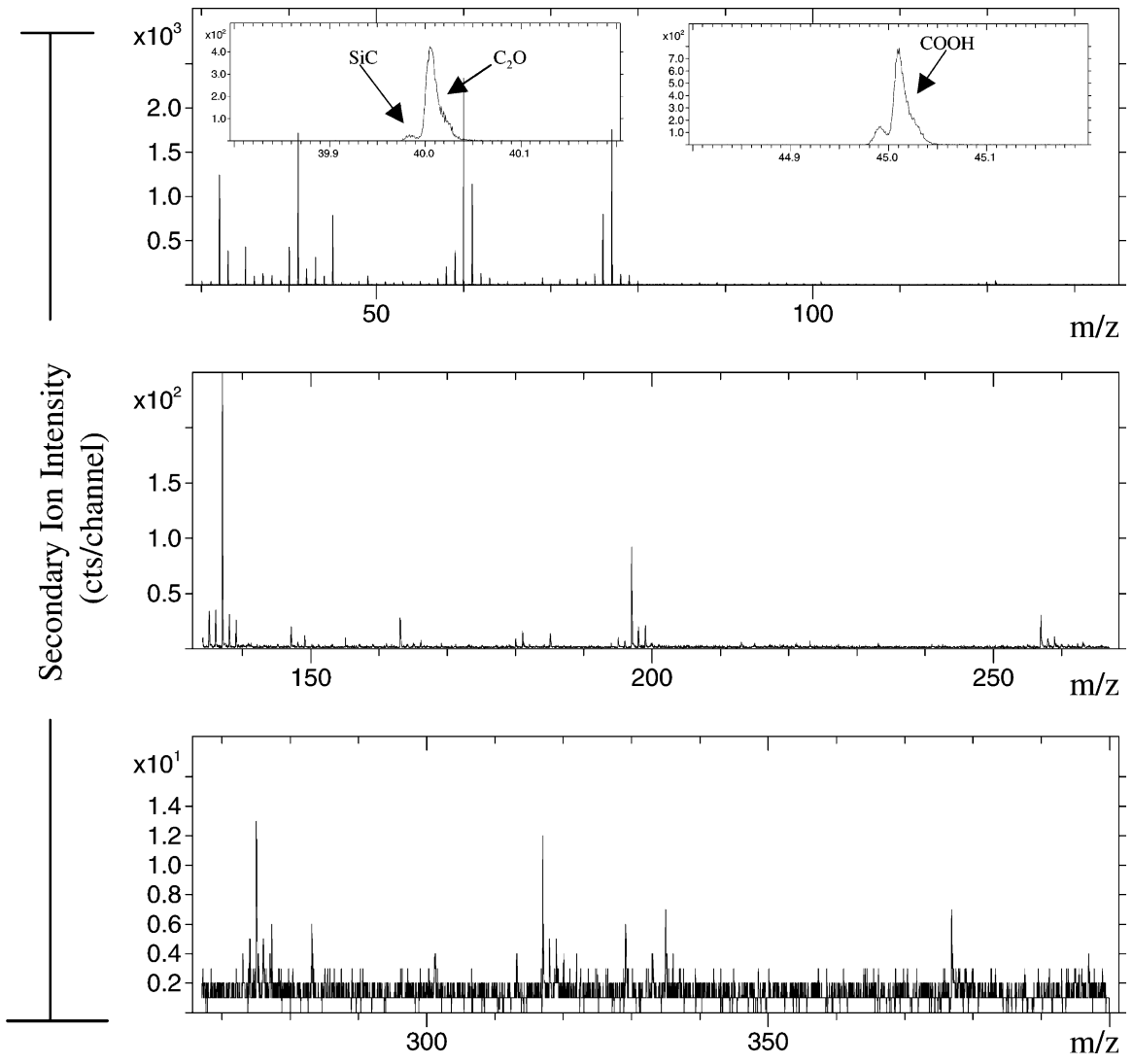


Fig. 6. High-mass-resolution negative ion SIMS spectrum of an irradiated OTS monolayer. The inset shows the peak intensities for $SiC^-$ and $C_2O^-$ (*m*/*z* 40) and $COOH^-$ (*m*/*z* 45).

during the automated acquisition of 40 SIMS spectra. The stage was translated in 1.00 mm increments. These spectra were analyzed using the IonSpec® software and are plotted from the least to the most hydrophilic end of the sample. The signals for the oxidized species, $SiOH^+$ and $Si_2O^+$, increase with the increasing hydrophilic nature of the surface as would be expected from the contact angle data shown in Fig. 1. The $SiCH_3^+$ signal, however, decreases as the surface becomes increasingly hydrophilic. This observation is also expected because the Si–$CH_3$ bond (see Fig. 2) fragments during UVO treatment.

Fig. 8 shows the negative secondary ion trends observed for $O^-$, $C_3^-$, and $COOH^-$ on the OTS sample. The stage was translated in 0.50 mm increments during the collection of the 80 spectra. These spectra were subjected to analysis with the custom program and, as described previously, are plotted from the least to the most hydrophilic end of the sample. The signal for $O^-$ increases with increasing UVO

exposure. The $C_3^-$ signal increases with the decreasing UVO exposure (decreasing hydrophilicity). This change is also attributed to fragmentation of the carbon chain caused by increasing exposure. The signal for $COOH^-$ also increases with increasing UVO exposure. UVO treatment produces atomic oxygen. In the UVO treatment of polymers, the atomic oxygen is thought to react with the carbon chain through insertion or hydrogen-abstraction reactions to produce oxidized entities, such as carbonyl and

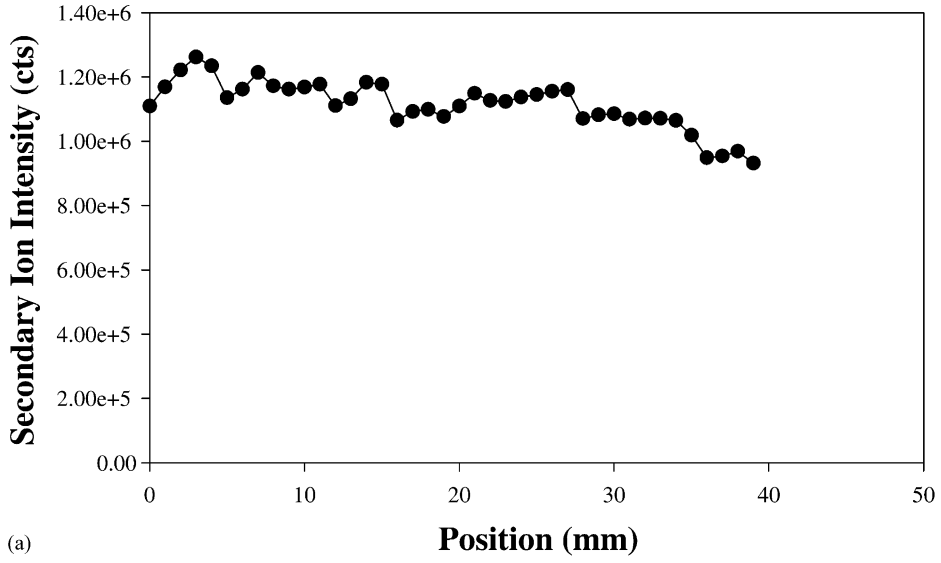


(a)

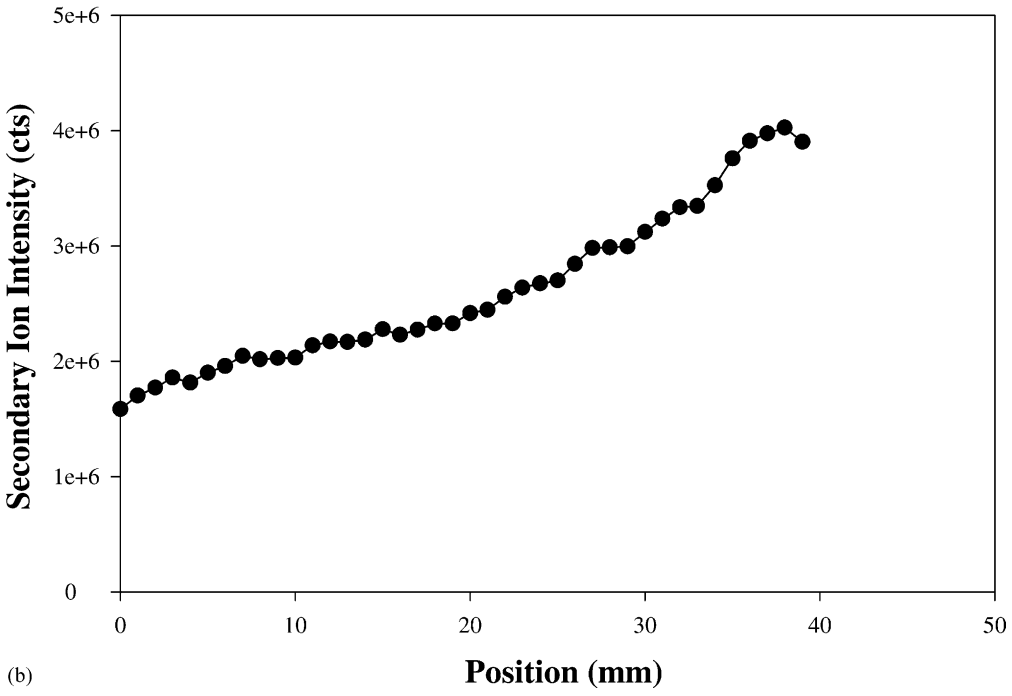


(b)

Fig. 7. Positive secondary ion trends observed along the length of the ODS sample—results for 40 spectra: (a) $SiCH_3^+$; (b) $SiOH^+$; (c) $Si_2O^+$.

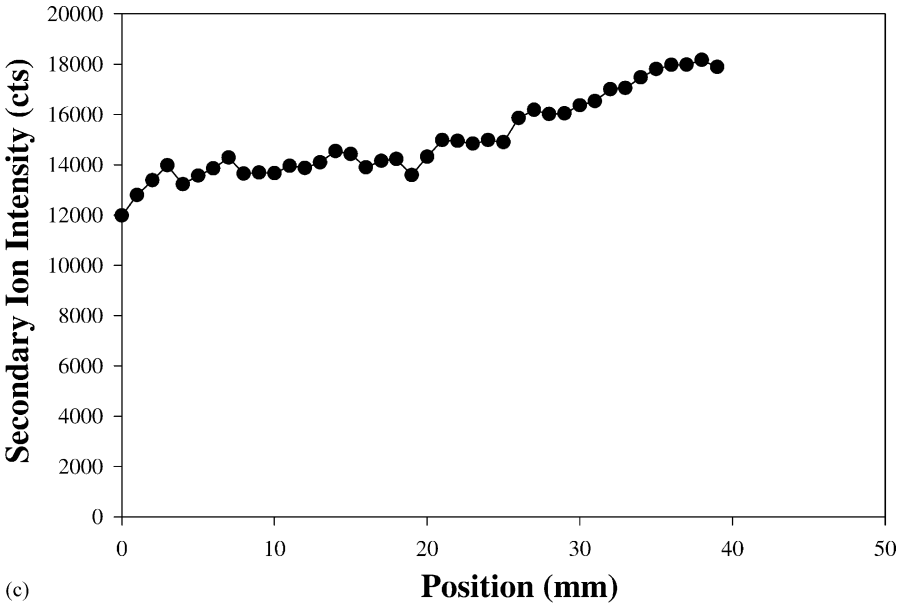


Fig. 7. (*Continued*).

carboxyl groups [15,20]. A similar mechanism likely comes into play with the carbon chain of the silane monolayer. The signals observed at the most hydrophilic end of the sample do not follow the expected trend. We would expect the signals for $O^-$ and $COOH^-$ to continue to increase at this end of the sample. Instead, these signals start to decrease. This behavior results because the UVO radiation was obstructed by a glass slide that was used to anchor this sample. This glass slide covered ≈10 mm (20, 0.5 mm steps) of the sample edge.

The thickness of the monolayer samples under investigation is ≈1.2 nm. This estimate is based upon the length of the C-8 aliphatic chain [24]. From SRIM [25] simulations, we estimate that the penetration depth of the incoming 9 keV $Ar^+$ beam into the sample is 25 nm. Although this depth is substantially greater than the thickness of the monolayer, the information depth (escape depth for ions) in SIMS is known to be on the order of 1 nm [26]. To determine to what, if any extent, the observed secondary ion signals were affected by the signal from the underlying $SiO_2$/Si substrate, data was also collected from a bare silicon wafer. The wafer was exposed to UVO treatment for 10 min. The surface was then etched with HF, and the oxide layer was re-grown with a 3 min UVO exposure. A 5 min exposure through the variable density filter followed. The signal for $SiOH^+$ was tracked in 4 mm steps along the wafer. Fig. 9 shows a plot of this data. The $SiOH^+$ signal is relatively constant, with a relative standard deviation (R.S.D.) of 4.2%. By contrast, the R.S.D. for $SiOH^+$ on the ODS gradient sample was ≈25%. This finding indicates that the observed trends originate from the silane monolayers and are only marginally affected by the underlying substrate.

Instrumental effects can also influence secondary ion signals, as ion collection efficiency may be influenced by instrumental geometry and may vary as a function of stage position [27]. To rule out this effect, the variations in secondary ion intensities as a function of sample stage position were addressed. The $SiOH^+$ signal from an irradiated and an unirradiated OTS monolayer was monitored. (The variable density filter was not utilized during these exposures.) Three measurements were taken at different positions on each of the samples, avoiding the edges of the silicon wafer. (Data not shown.) The R.S.D. for the $SiOH^+$ signal of the unirradiated sample was 4.1%, while that for the irradiated sample was 0.50%. These results suggest that the stage position has a minimal effect on the signals that were observed. Similar data were obtained for other peaks.

Numerous samples were prepared and analyzed in this study. The plots shown in the paper are representative plots. Because the trend analyses took place over periods of 4–8 h, it was not feasible to perform multiple runs on different spots for the purpose of monitoring the reproducibility of the technique. Nor was it possible to make multiple measurements in the same spot because we would have exceeded the static

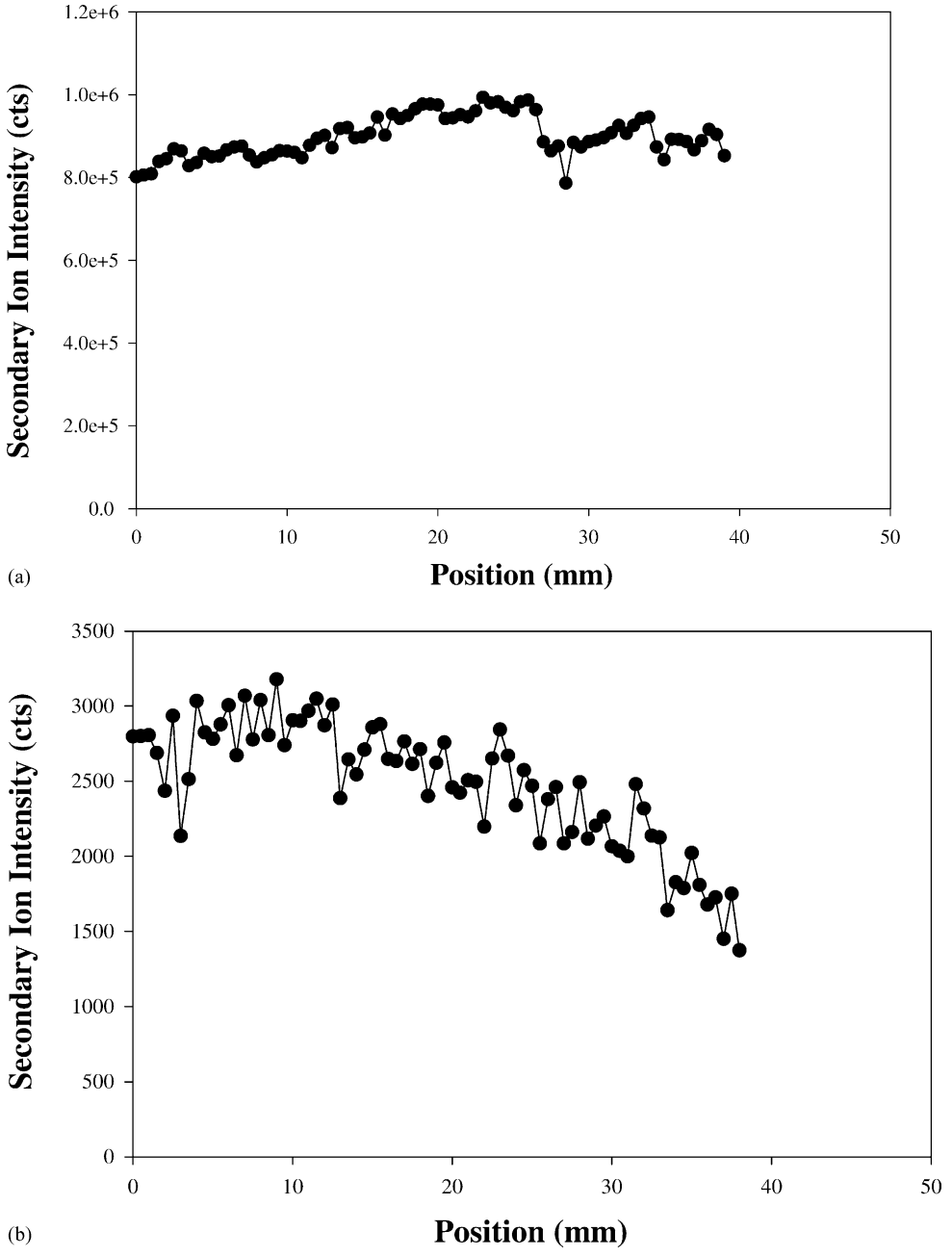


Fig. 8. Negative secondary ion trends observed along the length of the OTS sample—results for 80 spectra: (a) $O^-$; (b) $C_3^-$; (c) $COOH^-$. Each step represents 0.5 mm.

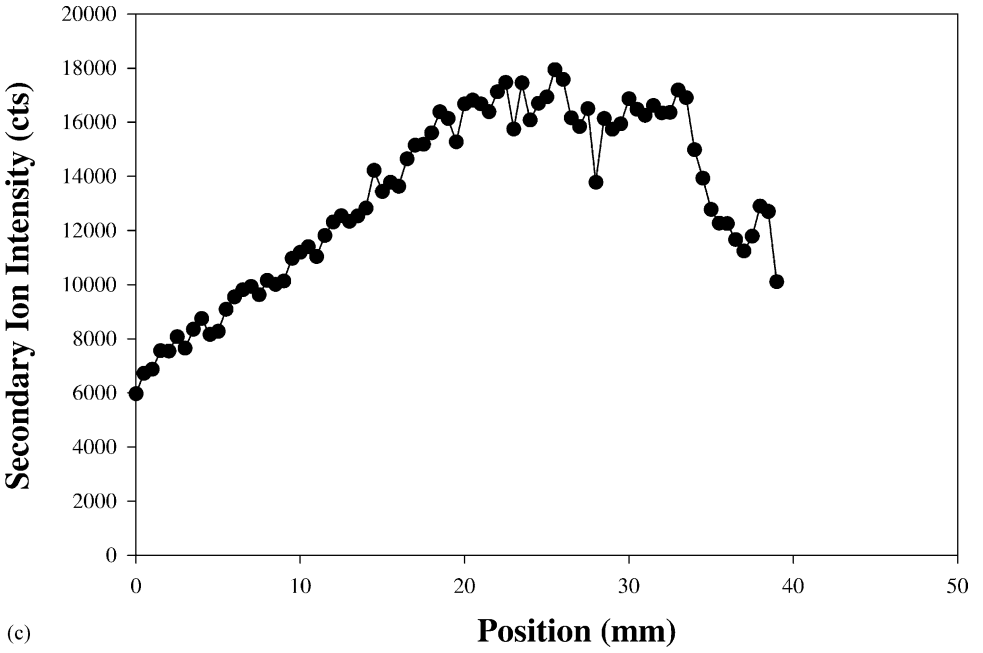


Fig. 8. (*Continued*).

SIMS (SSIMS) or low-dose SIMS limit of $10^{13}$ ions/cm$^2$. In addition, although all of the data exhibited trends qualitatively similar to the ones shown in Figs. 7 and 8, absolute secondary ion yields for different samples, prepared on different days, varied significantly. The reproducibility of absolute secondary ion intensities is not the most critical issue to be considered with these measurements. The variability between the

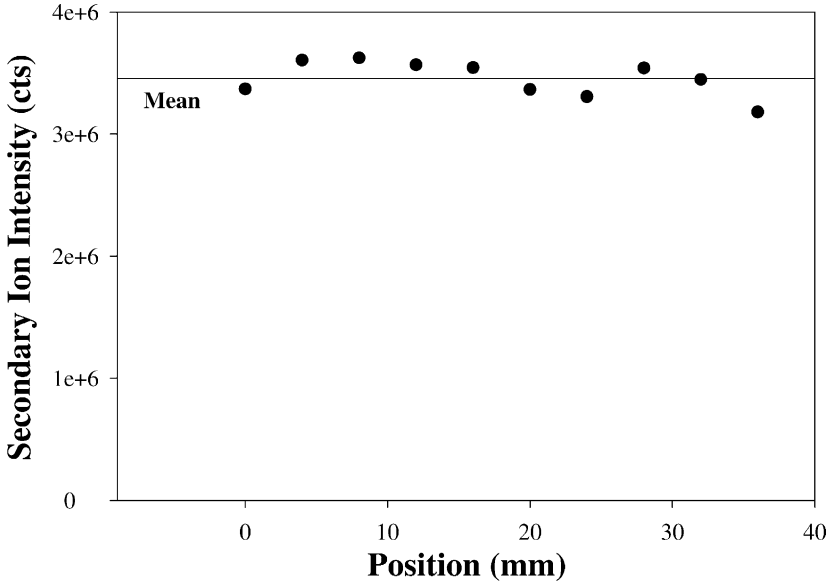


Fig. 9. Plot of $SiOH^+$ signal on a UVO (gradient) exposed silicon wafer.

minimum and maximum values in the trend plots is a more critical issue. For the data shown in Figs. 7 and 8, the $COOH^-$ exhibited the most pronounced difference. The minimum and maximum values for this signal were compared for four samples. The ratio of the maximum to minimum values had a mean of 2.5 and an R.S.D. of 24%. The $SiOH^+$ signal showed more variation, with a mean of 2.3 and an R.S.D. of 38%. We have also found that the secondary ion intensity ratios are quite dependent upon the humidity conditions under which the samples are prepared.

### 3.4. Secondary ion imaging

Molecule-specific imaging is one of the major strengths of ToF-SIMS. It is now possible to obtain image resolution approaching 200 nm with a $Ga^+$ ion probe from a liquid metal ion source. Another strength of ToF-SIMS is its parallel imaging capabilities. This characteristic, coupled with the high spatial resolution, has the potential to allow for very rapid screening of combinatorial arrays. To illustrate this point, a patterned monolayer was prepared. An aluminum mask (500 μm spacing between adjacent grid bars) was positioned over a portion of the monolayer; the mask was secured by means of a stainless steel ring. The monolayer was then exposed to UVO treatment for 10 min. Fig. 10 shows positive and negative, mass-specific secondary ion images obtained from the surface. The area that the mask protected from UVO exposure shows differential secondary ion intensities (for each ion monitored) as compared to the exposed

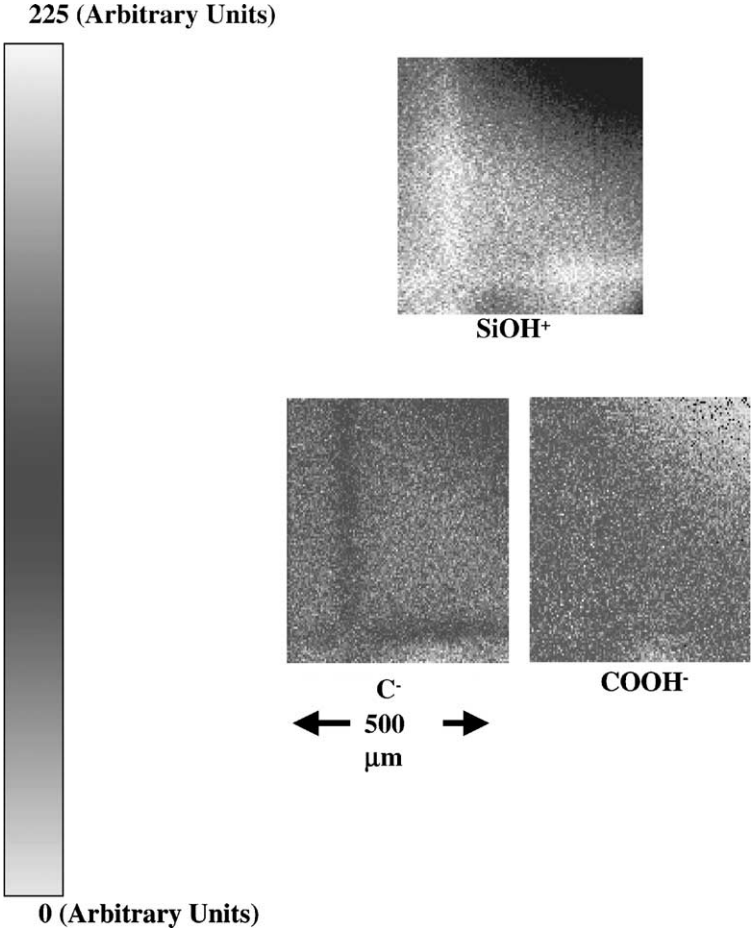


Fig. 10. Secondary ion images of a patterned OTS sample.

region. The signals for $SiOH^+$, $C^-$ and $COOH^-$ are shown. (Acquisition times ranged from 534 to 1047 s.)

## 4. Conclusions

The surface chemistry of silane monolayers can be modified by UVO treatment.

There is a direct relationship between increased hydrophilicity (increasing surface energy values) and the presence of oxygenated functional groups. Conversely, there is an inverse relationship between the degree of hydrophilicity and the secondary ion signals associated with intact C–C and Si–C bonds. The secondary ion signals for $SiC^-$, $C_3^-$ and $SiCH_3^+$ decreased as the level of UVO exposure increased. Concomitant with these findings, increases in the signals for $Si_2O^+$ and $C_2O^-$ were observed. The data suggest that UVO treatment causes not only bond breaking but cross-linking of the ODS and OTS monolayers as well. These secondary ion intensities can be employed not only to characterize the surfaces, but also for imaging purposes. The differential secondary ion intensities of exposed versus unexposed areas provide a contrast mechanism and illustrate that the surfaces can be patterned with regions of varying chemical functionality, a finding that could prove useful in various combinatorial assays.

## Acknowledgements

We acknowledge Dr. Christopher Soles for performing the X-ray reflectivity experiments.

## References

[1] E. Danielson et al., Nature 389 (1997) 944–948.
[2] E. Danielson et al., Science 279 (1998) 837–839.
[3] E. Reddington et al., Science 280 (1998) 1735.
[4] X.-D. Sun, Appl. Phys. Lett. 72 (1998) 525.
[5] X.-D. Xiang et al., Science 268 (1995) 1738.
[6] J. Wang et al., Science 279 (1998) 1712.
[7] S. Brocchini, K. James, V. Tangpasuthadol, J. Kohn, J. Am. Chem. Soc. 119 (1997) 4553.
[8] S. Brocchini, K. James, V. Tangpasuthadol, J. Kohn, J. Biomed. Mater. Res. 42 (1998) 66.
[9] T.A. Dickinson, D.R. Walt, J. White, J.S. Kauer, Anal. Chem. 69 (1997) 3413.
[10] B. Jandeleit, D.J. Schaefer, T.S. Powers, H.W. Turner, W.H. Weinberg, Angew. Chem. Int. Ed. 38 (1999) 2494.
[11] P.G. Schultz, X.-D. Xiang, Curr. Opin. Solid State Mater. Sci. 3 (1998) 153–158.
[12] A.P. Smith, J.F. Douglas, J.C. Meredith, E.J. Amis, A. Karim, Phys. Rev. Lett. 8701 (1) (2001) 015503-1–015503-4.
[13] J.C. Meredith, A.P. Smith, A. Karim, E.J. Amis, Macromolecules 33 (26) (2000) 9747–9756.
[14] H.Y. Nie, M.J. Alzak, B. Berno, N.S. McIntyre, Appl. Surf. Sci. 144/145 (1999) 627–632.
[15] D.O.H. Teare, C. Ton-That, R.H. Bradley, Surf. Interface Anal. 29 (2000) 276–283.
[16] L.A. Girifalco, R.J. Good, J. Phys. Chem. 61 (1957) 904.
[17] L.A. Girifalco, R.J. Good, J. Phys. Chem. 64 (1960) 561.
[18] K. Ashley, A. Sehgal, E.J. Amis, D. Raghavan, A. Karim, Combinatorial Mapping of Polymer Film Wettability on Gradient Energy Substrates, manuscript in preparation.
[19] M. Ouyang, C. Yuan, R.J. Muisener, A. Boulares, J.T. Koberstein, Chem. Mater. 12 (2000) 1591–1596.
[20] T. Ye, D. Wynn, R. Dudek, E. Borguet, Langmuir 17 (2001) 4497–4500.
[21] T.K. Kim, X.M. Yang, R.D. Peters, B.H. Sohn, P.F. Nealey, J. Phys. Chem. B 104 (2000) 7403–7410.
[22] A. Tóth, I. Bertóti, G. Marletta, G. Ferenczy, M. Mohai, Nucl. Instrum. Methods Phys. Res. Sect. B 116 (1996) 299–304.
[23] A. Licciardello, Universita' di Cantania, personal communication, 27 March 2001.
[24] A. Ulman, An Introduction to Ultrathin Organic Films—From Langmuir–Blodgett to Self-Assembly, Academic Press, Boston, 1991, pp. 283–284.
[25] J.F. Ziegler, J.P. Biersack, U. Littmark, in: J.F. Ziegler (Ed.), The Stopping Range of Ions in Matter, Pergamon Press, New York, 1985.
[26] A. Benninghoven, F.G. Rüdenauer, H.W. Werner, Secondary Ion Mass Spectrometry, Wiley, New York, 1987, pp. 874–875.
[27] J.C. Vickerman, A. Brown, N.M. Reed (Eds.), Secondary Ion Mass Spectrometry: Principles and Applications, Oxford University Press, New York, 1989, pp. 253–255.